

Structure Function Measurements at HERA and Perturbative QCD

Gregorio Bernardi

on behalf of H1 and ZEUS collaborations ¹

LPNHE-Paris, 4 place Jussieu, 75252 Paris Cedex 05, France

Abstract

New results from the H1 and ZEUS collaborations on the measurement of cross-sections at very high Q^2 (up to 25000 GeV²) and on the proton structure function $F_2(x, Q^2)$ for momentum transfers squared $Q^2 \geq 1.5$ GeV² and Bjorken $x \geq 3.5 \cdot 10^{-5}$ are reported, using data collected at HERA mainly in 1994. No deviations from the Standard Model have been observed at high Q^2 and F_2 is seen to increase significantly with decreasing x , even in the lowest reachable Q^2 region. Comparisons at low Q^2 with fixed target experiments and with models based on pomeron exchange are presented. The F_2 results are well described by a Next to Leading Order QCD fit, and are consistent at the present level of precision with the rise at low x within this Q^2 range generated via the DGLAP evolution equations. The gluon density is extracted and being observed to rise at low x .

1 Introduction

The HERA ep collider has been designed to study Deep Inelastic Scattering (DIS) at very high Q^2 , where the strength of the electromagnetic and weak forces become comparable and where substructure of quarks might be observed. However in the first 3 years of data operation, which allowed a steady growth towards the design luminosity of the machine, most of the interest has focused on the study of low x , low Q^2 DIS, where new tests of perturbative QCD can be performed. The first observations on the 1992 data showed a rise of the proton structure function $F_2(x, Q^2)$ at low $x < 10^{-2}$ with decreasing x [6, 7], which was confirmed with the more precise data of 1993 [8, 9]. Such a behaviour is qualitatively expected in the double leading log limit of Quantum Chromodynamics [10]. It is, however, not clarified whether the linear QCD evolution equations, as the conventional DGLAP evolution [11] in $\ln Q^2$ and/or the BFKL evolution [12] in $\ln(1/x)$, describe the rise of F_2 or whether there is a significant effect due to non-linear parton recombination [13]. At low Q^2 (≤ 5 GeV²) the new results can be confronted with Regge inspired models, which expect a rather flat behaviour as a function of x , in order to study the transition between

¹Invited plenary talk given at Baryons '95 held in Sante Fé, New Mexico, in October 1995. The results presented here have been updated according to the recent publications of ZEUS [1], H1 [2, 3] and E665 [4]. Original figures can be found for instance in [5].

DIS and photoproduction. The 1994 data have made possible to reach an extended kinematic region, both in Q^2 and in x , and to confirm the persistence of the rise at low x at the lowest Q^2 measured. The very high Q^2 results are presented in section 1. The latest F_2 measurements which have been achieved by using dedicated data samples are presented in section 2 and their low Q^2 behaviour is discussed in section 3. They are analyzed in terms of perturbative QCD in section 4.

2 Differential Cross-Sections at Very High Q^2

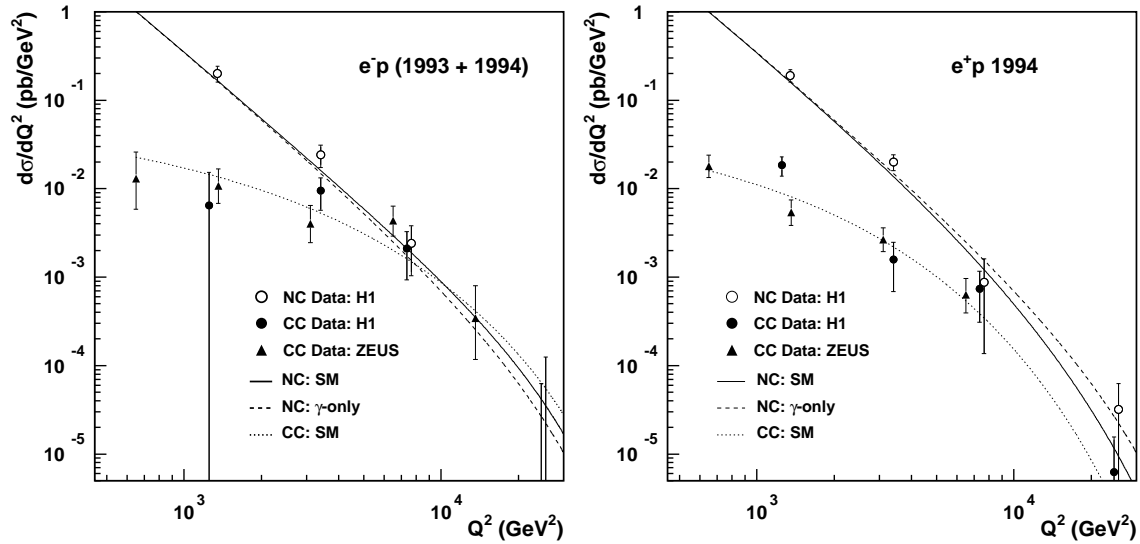


Figure 1: Measurement of the Born differential cross-section $d^2\sigma/dQ^2$ by the H1 and ZEUS collaborations for NC and CC in e^-p (a) and e^+p (b) collisions.

At very high Q^2 , i.e. when $Q^2 \simeq M_W^2$, the electroweak unification is expected to become visible. At HERA, both charged (CC : $ep \rightarrow \nu X$) and neutral currents (NC : $ep \rightarrow eX$) are easily selected by requesting that the global momentum transfer of the hadronic final state is large, typically ≥ 20 GeV. The separation between CC and NC is based on the detection of the charged scattered lepton present only in the NC events. In 1993 and 1994 a luminosity of about $0.8 pb^{-1}$ of e^-p and $3 pb^{-1}$ of e^+p collisions have been recorded allowing new tests of the Standard Model. The CC differential cross-sections can be written in leading order as

$$\frac{d^2\sigma_{CC}^{e^-}}{dQ^2} = \frac{G}{(1 + Q^2/m_{W^-}^2)^2} [u + c + (1 - y)^2(\bar{d} + \bar{s} + \bar{b})] \quad (1)$$

$$\frac{d^2\sigma_{CC}^{e^+}}{dQ^2} = \frac{G}{(1 + Q^2/m_{W^+}^2)^2} [d + s + b + (1 - y)^2(\bar{u} + \bar{c})] \quad (2)$$

where G is a coupling constant, m_{W^\pm} are the masses of the charged weak bosons, and u, d, c, s, b , are the quark densities in the proton. In fig. 1 the measurement of these differential cross-sections are displayed and shown to be of a similar strength as the NC one,

when at high Q^2 . A shape and magnitude analysis of these distributions allows the determination of the masses of the propagators involved. M_{W^+} and M_{W^-} are found to be consistent, and a combined fit results in a mass $m_W = 84_{-7}^{+10}$ GeV (H1, [3]) or 79_{-7}^{+10} GeV (ZEUS, preliminary), both compatible with the precise measurement made at $p\bar{p}$ colliders where W's are directly produced. The statistical error is still the dominant source of the total error given on M_W since only about 200 CC events have been recorded at HERA in 1993-94. The effect of the Z^0 vector boson is not yet distinguishable from the single photon exchange cross-section, as shown in fig. 1. With the expected higher luminosity, the ratio u/d and the structure function xF_3 will be determined, while unexpected deviations from the Standard Model could reveal new insights in the deepest structure of matter.

3 Structure Function Measurement at HERA

In 1994 the H1 and ZEUS experiments have reduced the minimum Q^2 at which they could measure F_2 using several techniques: i) by diminishing the region around the backward beam pipe in which the electron could not be measured reliably in 1993, the maximum polar angle of the scattered electron (measured with respect to the proton beam direction) was increased. The integrated luminosity of this large statistic sample is about 3 pb^{-1} . ii) DIS events which underwent initial state photon radiation detected in an appropriate photon tagger were used to measure F_2 at lower Q^2 (so called "radiative" sample) since the incident electron energy in the hard scattering is reduced. iii) A luminosity of $\sim 60 \text{ nb}^{-1}$ of data was collected for which the interaction point (vertex) was shifted by about +65 cm, in the forward direction, resulting in an increase of the electron acceptance (so-called "shifted vertex" data sample). The precision of these luminosity measurements are based on the Bethe-Heitler reaction $e^-p \rightarrow e^-p\gamma$ and is 1.5% (3 to 4% for the shifted vertex and radiative data).

The kinematic variables of the inclusive scattering process $ep \rightarrow eX$ can be reconstructed in different ways using measured quantities from the hadronic final state and from the scattered electron. The choice of the reconstruction method for Q^2 and y determines the size of systematic errors, acceptance and radiative corrections. The measurements presented here have been obtained with the electron method (E), with the Σ method [14], and with a combination of the double-angle (DA) [15] and Σ method. The E method has at large y the best resolution in x and Q^2 but needs sizeable radiative corrections and cannot be used at low y due to the degradation of the y resolution as $1/y$. The Σ method, which has small radiative corrections, relies mostly on the hadronic measurement and can be used from very low to large y values. H1 measures F_2 with the E and the Σ method and after a complete consistency check, in particular at low x , uses the E method for $y > 0.15$ and the Σ method for $y < 0.15$. ZEUS measures F_2 from the shifted vertex and radiative data with the E method, otherwise with the Σ -DA combination.

The event selection is similar in the two experiments. Events are filtered on-line using calorimetric triggers which request an electromagnetic cluster of at least 5 GeV not vetoed by a trigger element signing a beam background event. Offline, further electron identification criteria are applied (track-cluster link, shower shape and radius) and a minimum

energy of about 10 GeV is required. H1 requests a reconstructed vertex within 3σ of the expected interaction position, while ZEUS requires, in order to reduce the photoproduction background and the size of the radiative corrections, that $35 \text{ GeV} < \Sigma + E'_e(1 - \cos \theta) < 65 \text{ GeV}$. The only significant background left after the selection comes from photoproduction in which a hadronic shower or a photon fakes an electron. In H1 for instance, it amounts to less than 3% except in a few bins where it can reach values up to 15%. It is subtracted statistically bin by bin and an error of 30% is assigned to it.

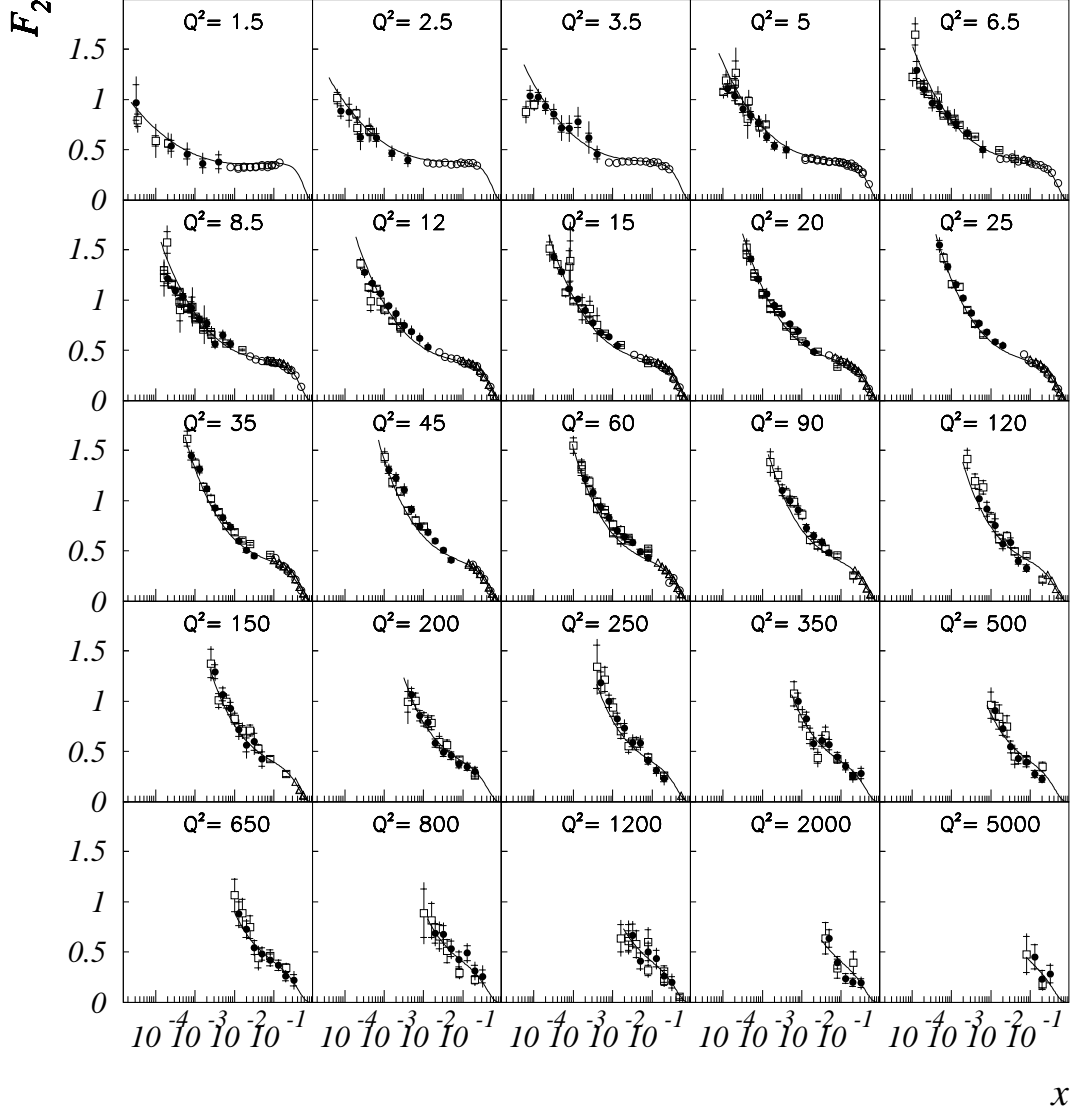


Figure 2: $F_2(x, Q^2)$ measurement as a function of x by H1 (black circles, [2]), ZEUS (open squares, preliminary, except at low Q^2 [1]), NMC (open circles, [19]), BCDMS (open triangles, [20]). The curve represent the GRV model prediction.

The acceptance and the response of the detector have been studied and understood in great detail by the two experiments: more than two million Monte Carlo DIS events,

corresponding to an integrated luminosity of approximately 20 pb^{-1} , were generated with DJANGO [16] using the GRV [17] and MRS [18] parametrizations of the parton distributions. The Monte Carlo events, after a detailed detector simulation were subjected to the same reconstruction and analysis chain as the real data.

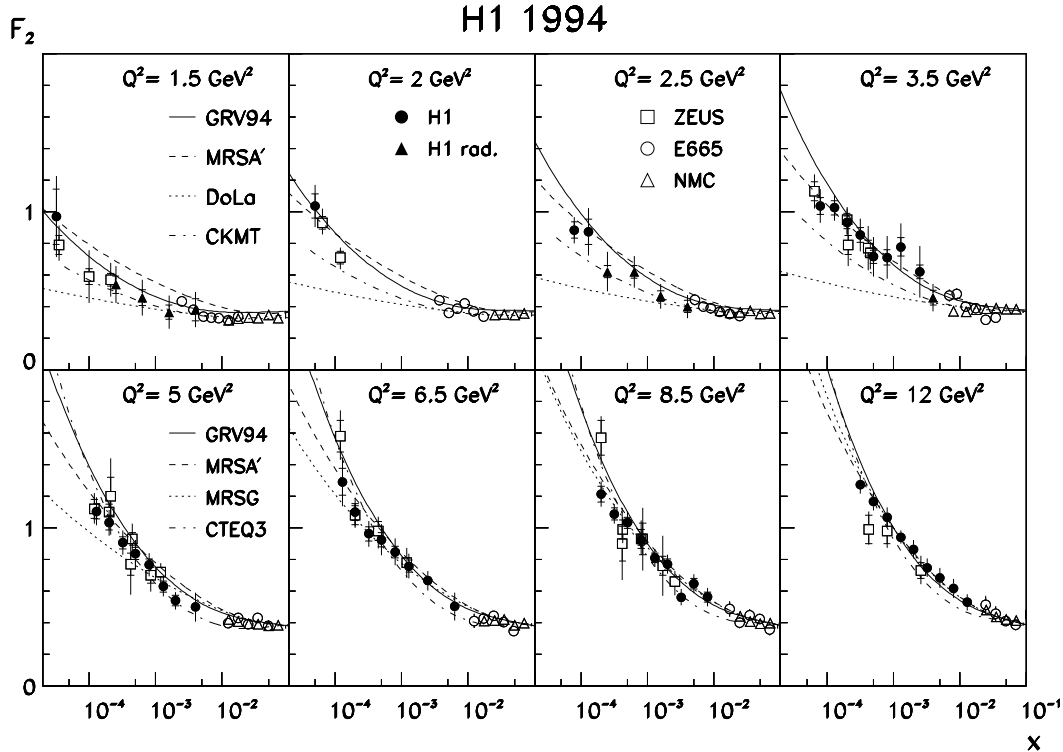


Figure 3: $F_2(x, Q^2)$ measurement in the low Q^2 region by H1 and ZEUS compared to the results of the E665 and NMC fixed target experiments. The F_2 parametrizations confronted to the data and discussed in the text are DOLA and CKMT at $Q^2 < 5 \text{ GeV}^2$, GRV and MRSA'.

The structure function $F_2(x, Q^2)$ was derived after radiative corrections from the differential cross-section $d^2\sigma/dxdQ^2$. ($R \equiv F_2/2xF_1 - 1$ was taken as prescribed by QCD). With the different data sets available, detailed cross checks could be made in the kinematic regions of overlap. The results were found to be in very good agreement with each other for all kinematic reconstruction methods used, and the effect of systematic errors could be monitored. For the E method the main source of error are the energy calibration (known at the 1% level), the knowledge of the electron identification efficiency, the error on the polar angle of the scattered electron (1 mrad), and the radiative corrections at low x . The DA method becomes strongly sensitive to the precision of the of the electron and hadronic angle when they tend to their boundary values (0 or π). For the Σ method, the knowledge of the absolute energy scale for the hadrons, the fraction of hadrons which stay undetected, in particular at low x , due to calorimetric thresholds and to a lesser extent the electron energy calibration are the dominating contributions. The total F_2 errors on the 1994 data ranges between 5 and 10% in the 10-100 GeV^2 range and between 10 and 20% below 10

GeV². The final results from the 1994 data of H1 and ZEUS are shown in fig. 2. Compared to the 1993 data analyses the F_2 measurement has been extended to lower x (from $1.8 \cdot 10^{-4}$ to $3.5 \cdot 10^{-5}$) and in Q^2 (from 4.5-1200 GeV² to 1.5-5000 GeV²). Both experiments are in good agreement and show that the F_2 rise at low x persists, albeit less strongly, down to the lowest measured $Q^2=1.5$ GeV². A smooth transition between the HERA data and the results of the fixed target experiments NMC [19] and BDMCS [20] is observed, and for the first time also at low $Q^2 \leq 5$ GeV² between E665 [4] and the low y results of H1 (fig 3), allowing these consistent results to be confronted with theoretical expectations.

4 Structure Functions at Low Q^2

In fig. 3 we focus on the low Q^2 measurements, i.e. in the new kinematic domain reached using the radiative and the shifted vertex data. Also shown are the extrapolations of the F_2 parametrizations based on theoretical models adjusted to the previous data. They can be divided in two categories: one, motivated by Regge theory, assumes pomeron exchange as a dynamical basis and successfully describes the behaviour of the total cross-sections of photoproduction and hadron-hadron collisions; the other is based on perturbative QCD and is known to describe well the evolution of the DIS cross-sections, but is expected to fail at some low Q^2 .

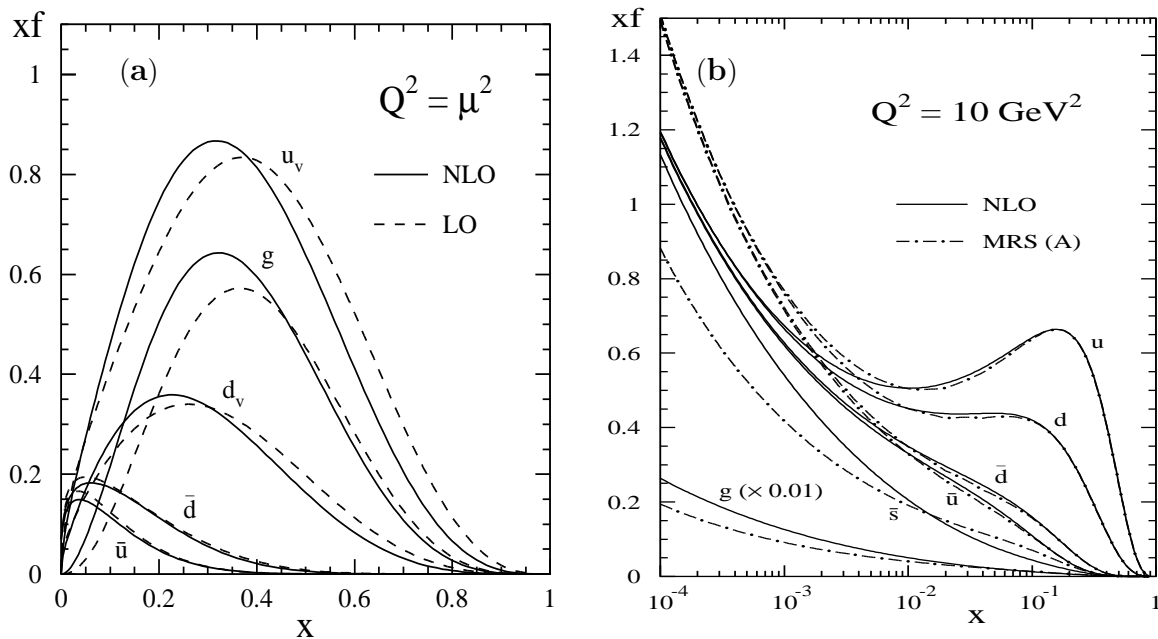


Figure 4: a) Parton densities (valence quarks (u_v, d_v), gluon (g) and sea quarks) of the GRV model at the initial energy scale $\mu^2 = 0.34$ GeV². b) at a scale of 10 GeV², and compared to MRS(A).

The Regge models were expected to work at least at low Q^2 , but the DOLA parametrization which uses a “soft” pomeron (intercept $\simeq 1.08$) [21] largely underestimates F_2 at low x even at 1.5 GeV². The CKMT model [22], which assumes that in the present Q^2 range

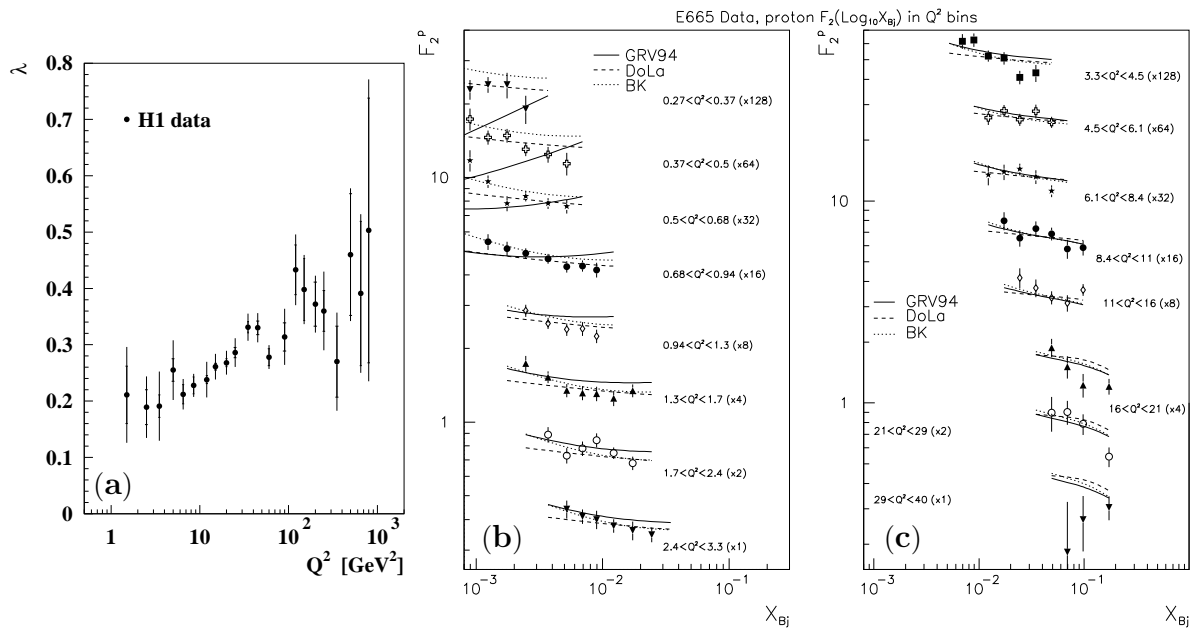


Figure 5: a) Variation of λ obtained from fits of the form $F_2 \sim x^{-\lambda}$ to the H1 data, at fixed Q^2 and $x < 0.1$. b), c) $F_2(x, Q^2)$ measurement in the low Q^2 region by the E665 experiment. Different F_2 parametrizations are confronted to the data: DOLA, BK and GRV (see text).

the “bare” pomeron becomes visible and has a higher trajectory intercept ($\simeq 1.24$), predicts a weaker rise at low x than observed, except maybe at 1.5 GeV². These comparisons underline the difference between the behaviour of the total cross-section of real and virtual photons, since in the HERA kinematic domain $\sigma_{tot}^{\gamma^*p}$ can be expressed as

$$\sigma_{tot}^{\gamma^*p}(x, Q^2) \simeq (4 \pi^2 \alpha / Q^2) \cdot F_2(x, Q^2). \quad (3)$$

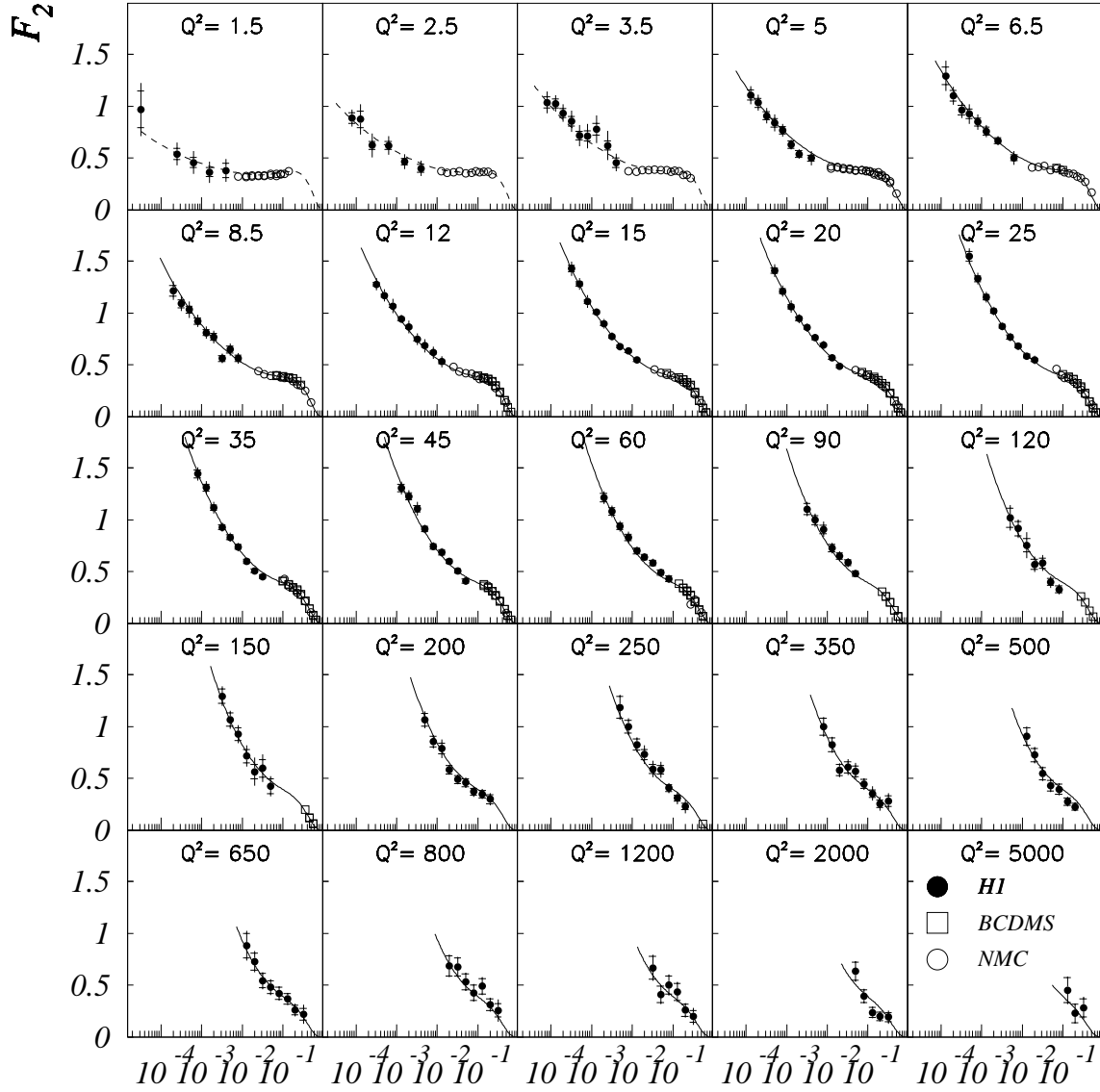
The parametrizations based on the DGLAP QCD evolution equations describe the data remarkably well, as expected above 5-10 GeV², but also surprisingly at values around 1 or 2 GeV² where non-perturbative effects were believed to distort the DGLAP picture. The MRSA’ parametrizations of the parton densities are defined at $Q_0^2 = 4$ GeV², then evolved in Q^2 and fitted to previous experimental data, including the 1993 HERA data. The agreement observed above 10 GeV² confirms that the 1993 and 1994 HERA results are perfectly compatible. Between 1.5 and 10 GeV² the good description tells us that within the present precision perturbative QCD can be applied in this range. More striking is the confirmation of the pre-HERA prediction of the F_2 rise at low x by the GRV model [17] which conjectured that at a very low energy scale ($\mu^2 = 0.34$ GeV²) the proton is formed by valence-like partons as shown in fig. 4a and that the DGLAP equations can be applied to generate “radiatively” the rise of the gluon and sea-quark density at low x , when evolving towards higher Q^2 (fig. 4b). The H1 and ZEUS results are well described by the GRV model as can be seen in fig. 2 and 3. This success supports the idea that the rise at low x is a direct consequence of the DGLAP equations, and that non-perturbative effects are relatively weak at low x and low Q^2 .

The evolution with Q^2 of the strength of the rise can be quantified by fitting an $x^{-\lambda}$ function (or equivalently a form $W^{2\lambda}$, W being the invariant mass of the $\gamma^* - p$ system, as shown in [23]) at fixed Q^2 to $F_2(x)$, $x < 0.1$. The values of λ obtained by the fit in each Q^2 bin are displayed in fig. 5a and clearly confirm the prediction of many years' standing made for asymptotic free field theories like QCD [10] of a rise of F_2 at low x , and that the size of this rise increases with Q^2 . With the present data, it is however not possible to know precisely this size below 5 GeV², thereby postponing a definite test of perturbative QCD in this region.

Recent results from the fixed target E665 experiment provide additional information, in particular below 5 GeV², while at $Q^2 \geq 5$ GeV² the E665 and NMC measurements are in good agreement (fig. 3). The x range however does not extend to the HERA values since its limit varies between 10^{-2} and 10^{-3} . In fig. 5b,c the E665 data are shown to be described in this medium x range and for $Q^2 > 0.3$ GeV² by the DOLA and BK [24] parametrizations, the latter being based on the concept of Generalized Vector Meson Dominance (GVMD) at low Q^2 with a smooth transition to perturbative QCD at higher Q^2 . At values below 0.7 GeV² the GRV description starts to break down, but the GRV approach is still valid below 1 GeV². The new HERA data taken in 1995 with upgraded detectors will further constrain these models at low x for $Q^2 < 1$ GeV² thereby checking if perturbative QCD can indeed explain the dynamics at these very low Q^2 .

5 Structure Functions and Perturbative QCD

To make full use of the new precision achieved with the 1994 data, the H1 collaboration has performed a Next-to-Leading Order (NLO) QCD fit on the H1, BCDMS and NMC data with the conditions $Q^2 > 5$ GeV², and $x < 0.5$ if $Q^2 < 15$ GeV² to avoid higher-twist effects. The H1 measurements which extend to 5000 GeV² were fitted successfully (fig. 6) and constrain the gluon density at low x . The parton densities were parametrized at $Q_0^2=5$ GeV², in particular the gluon was expressed with 3 parameters as $xg(x) = A_g x^{B_g} (1-x)^{C_g}$. The quark and antiquark components of the sea were assumed to be equal, and \bar{u} set equal to \bar{d} . As determined in [25], the strange quark density was taken to be $\bar{s} = (\bar{u} + \bar{d})/4$. Further constraints due to quark counting rules and momentum sum rules were included. For Λ the value of 263 MeV was taken [26]. A detailed treatment of the F_2 error propagation on the gluon density has been made, resulting in the error bands of fig. 7b which represent $xg(x)$ at 5 and 20 GeV². A variation of Λ by 65 MeV gives a change of 9% on the gluon density at 20 GeV² which has not been added to the error bands. The accuracy of this determination of xg is better by about a factor of two than the H1 result based on the 1993 data [27]. A rise of the gluon density towards low x is observed which is related to the behaviour of $F_2 \propto x^{-\lambda}$. Accordingly, the rise of xg towards low x increases with increasing Q^2 . Finally we can observe in fig. 6 that the data at $Q^2 < 5$ GeV², which were excluded from the fit, are still well reproduced by the fit evolved backwards in Q^2 . More data at low x and $Q^2 < 1$ GeV² are nevertheless needed to be able to test the hypothesis of a gluon density which would take the valence-like shape displayed in fig. 4a when $Q^2 \rightarrow 0.3$ GeV², and more generally, to better understand the dynamics at low Q^2 and low x were parton



x

Figure 6: $F_2(x, Q^2)$ measurement as a function of Q^2 . The curve represent a NLO QCD fit to the H1 (black circles), BCDMS (open squares) and NMC (open circles) data at $Q^2 > 5 \text{ GeV}^2$.

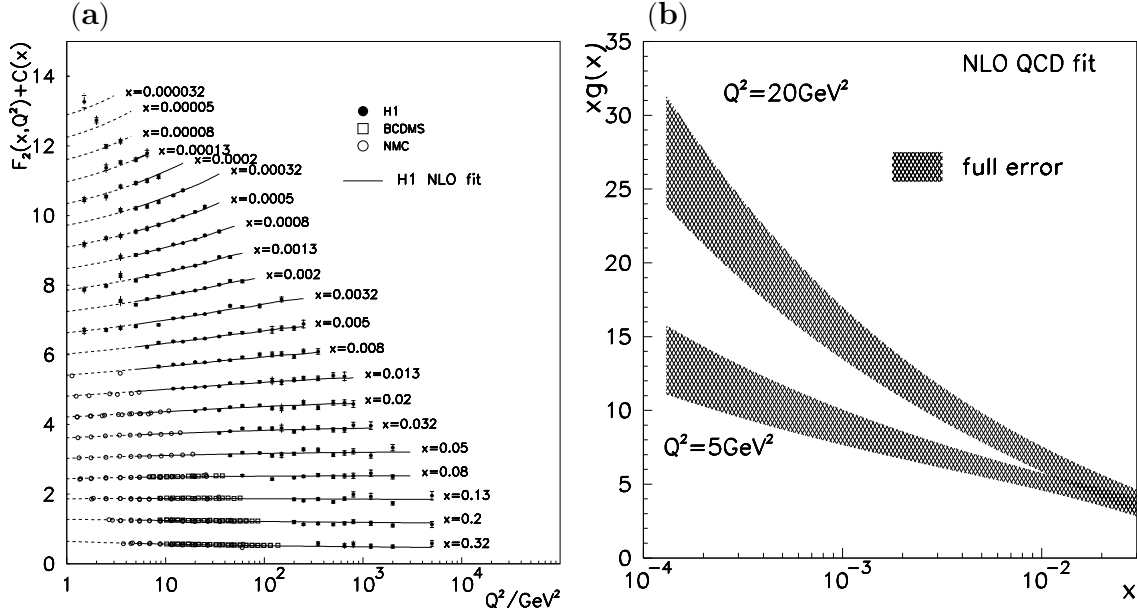


Figure 7: a) H1, BCDMS and NMC measurement of the proton structure function $F_2(x, Q^2)$ as function of Q^2 . The curve represent the NLO QCD fit to the H1, BCDMS and NMC data described in the text. b) Gluon density at 5 and 20 GeV^2 determined by a NLO fit to the H1, NMC and BCDMS data. The error bands represent the full error except for the uncertainty on Λ .

densities are high. The HERA experiments, which have last year upgraded their backward detectors, will be able to reach such low Q^2 with the data taken in 1995 and 1996.

In conclusion, the HERA 1994 data with their improved precision have provided new tests which have been passed successfully by perturbative QCD on 3 orders of magnitude in Q^2 , between 5 and 5000 GeV^2 . Another test not described in this report is the observation by the H1 collaboration [2] of double asymptotic scaling [28] as predicted by QCD, for Q^2 values above 5 GeV^2 . At the present level of precision the DGLAP evolution equations are sufficient to account for the observed rise of F_2 at fixed Q^2 , although it is not yet possible to distinguish between the different solutions of the “input” parton distribution problem which allow for a good description of the data. From 1.5 to 5 GeV^2 all analyses/interpretation of the F_2 behaviour hint that perturbative QCD is also applicable at these low Q^2 . However the lower statistical precision of these measurements obtained with dedicated data samples prevent a definite conclusion at the moment. The forthcoming 1995 results should have the precision and the extension at even lower Q^2 sufficient to constrain the limit of validity of perturbative QCD whose domain has been already observed to be wider than generally expected.

Acknowledgements

I would like to thank the organizers, particularly Ben Gibson, to have realized such an interesting conference in the nice town of Santa Fé. I would also like to thank my close collaborators, U. Bassler, B. Gonzalez-Pineiro and F. Zomer, J. Dainton for a careful reading of the manuscript, all the colleagues of the H1 structure function group in particular A. DeRoeck, J. Feltesse and M. Klein, and the E665, H1 and ZEUS collaboration with whom we obtained the recent results described above.

References

- [1] ZEUS Collab., M. Derrick et al., *Z. Phys.* **C69** (1996), 607.
The ZEUS results at higher Q^2 (nominal vertex) are preliminary as presented at the La Thuile conference in February 96.
- [2] H1 Collab., S. Aid et al., DESY 96-039 (1996), Subm. to *Nucl. Phys.*
- [3] H1 Collab., S. Aid et al., DESY 96-046 (1996), Subm. to *Phys. Lett.*
- [4] E665 Collab., M.R. Adams et al., *Phys. Rev. Lett.* **75** (1995) 1466.
- [5] F. Eisele, DESY-95-229, Proceedings of the 1995 International Europhysics Conference on High Energy Physics, Brussels.
- [6] H1 Collab., I. Abt et al., *Nucl. Phys.* **B407** (1993) 515.
- [7] ZEUS Collab., M. Derrick et al., *Phys. Lett.* **B316** (1993) 412.
- [8] H1 Collab., T. Ahmed et al., *Nucl. Phys.* **B439** (1995) 471.
- [9] ZEUS Collab., M. Derrick et al., *Z. Phys.* **C65** (1995), 379.
- [10] A. De Rújula et al, *Phys. Rev.* **D10** (1974) 1649.
- [11] Yu. L. Dokshitzer, *Sov. Phys. JETP* **46** (1977) 641;
V. N. Gribov and L.N. Lipatov, *Sov. J. Nucl. Phys.* **15** (1972) 438 and 675;
G. Altarelli and G. Parisi, *Nucl. Phys.* **B126** (1977) 297.
- [12] E. A. Kuraev, L. N. Lipatov and V. S. Fadin, *Sov. Phys. JETP* **45** (1977) 19; 9;
Y. Y. Balitsky and L.N. Lipatov, *Sov. J. Nucl. Phys.* **28** (1978) 822.
- [13] L. V. Gribov, E. M. Levin and M. G. Ryskin, *Phys. Rep.* **100** (1983) 1;
A. H. Mueller and N. Quiu, *Nucl. Phys.* **B268** (1986) 427.
- [14] U. Bassler and G. Bernardi, *Nucl. Instr. and Meth.* **A361** (1995) 197.
- [15] C. Hoeger, Proceedings of the Workshop Physics at HERA, vol. 1, eds. W. Buchmüller, G. Ingelman, DESY (1992) 43.
S. Bentvelsen et al., Proceedings of the Workshop Physics at HERA, vol. 1, eds. W. Buchmüller, G. Ingelman, DESY (1992) 23.

- [16] G. A. Schuler and H. Spiesberger, Proceedings of the Workshop Physics at HERA, vol. 3, eds. W. Buchmüller, G. Ingelman, DESY (1992) 1419.
- [17] M. Glück, E. Hoffmann and E. Reya, Z. Phys. **C13** (1982) 119.
M. Gluck, E. Reya and A. Vogt, Z. Phys. **C67** (1995) 433.
- [18] A.D. Martin, W.J. Stirling and R.G. Roberts, RAL preprint RAL-95-021 (1995).
- [19] NMC Collab., P. Amaudruz et al., Phys. Lett. **B259** (1992) 159.
- [20] BCDMS Collab., A. C. Benvenuti et al., Phys. Lett. **B237** (1990) 592.
- [21] A. Donnachie and P. V. Landshoff, Z. Phys. **C61** (1994) 139.
- [22] A. Capella et al., Phys. Lett. **B337** (1994) 358.
- [23] A. Levy, DESY 95-204 and hep-ex/9511006, Proceedings of the 1995 International Europhysics Conference on High Energy Physics, Brussels.
- [24] B. Badelek, J. Kiewcinski, Phys. Rev. **D50** (1994)
- [25] CCFR Collaboration, A.O. Bazarko et al., Z. Phys. **C65** (1995) 189.
- [26] M. Virchaux and A. Milsztajn, Phys. Lett. **B274** (1992) 221.
- [27] H1 Collab., S. Aid et al., Phys. Lett. **B354** (1995) 494.
- [28] R.D. Ball, S. Forte, Phys. Lett. **B335** (1994) 77.